

Collective Relaxation of Protein Protons at Very Low Magnetic Field: A New Window on Protein Dynamics and Aggregation

Claudio Luchinat* and Giacomo Parigi

Contribution from the Magnetic Resonance Center and Department of Agricultural Biotechnology, University of Florence, Via Maragliano 75/77, 50144 Florence, Italy

Received May 13, 2006; E-mail: luchinat@cerm.unifi.it

Abstract: Since the recent availability of high sensitivity field-cycling relaxometers, it has become possible to measure the protein proton relaxation in millimolar protein solutions as a function of magnetic field. In principle, this provides direct access to the so-called spectral density function of protein protons and, hence, to a full set of dynamic parameters. Understanding the dynamic behavior of biological molecules is increasingly appreciated as crucial to understanding their function. However, theoretical tools to analyze the collective relaxation behavior of protons in solute macromolecules over a wide range of magnetic fields are lacking. A complete relaxation matrix analysis of such behavior is described here. This analysis provides excellent predictions of the experimental proton magnetization decays/recoveries—measured to an unprecedented level of accuracy by a last-generation fast field-cycling relaxometer—of two different globular proteins, hen egg white lysozyme and human serum albumin. The new experimentally validated theoretical model is then used to extract dynamic information on these systems. A “collective” order parameter S_C^2 , different from, but complementary to, that commonly extracted from heteronuclear relaxation measurements at high field, is defined and measured. An accurate estimate of the rotational correlation time is obtained: in the case of lysozyme it agrees very well with theoretical predictions; in the case of serum albumin it provides evidence for aggregation at millimolar concentration.

Introduction

Nuclear relaxation rates are commonly used to extract information on protein mobility. The measurement of relaxation rates with high-resolution NMR, at one or a few magnetic fields, for a set of protein nuclei subject to known dominant relaxation mechanisms is a commonly used technique to investigate conformational heterogeneity and motional timescales in the different protein regions by looking at the tail of the appropriate spectral density functions.^{1–6} However, the measurement of collective protein proton relaxation rates over a wide field range (called relaxation dispersion profile) could in principle allow us to extract direct information on the entire protein proton spectral density and, thus, extract further information on protein dynamics.^{7,8}

Such measurements are now feasible,⁹ thanks to the availability of a high sensitivity field-cycling relaxometer,^{10–14}

recently developed.¹⁵ The latter can directly detect protein protons signals in millimolar protein solutions in D_2O ⁹ over a very wide field range (from a few kilohertz to a few tens of megahertz proton Larmor frequency), being thus able in principle to provide the relaxation dispersion profile of nuclei of proteins in solution, i.e., the “true” form of the spectral density $J(\omega, \tau)$, which is a function of the nuclear Larmor frequency, ω , and of the correlation time, τ , for the dipolar interactions. However, the magnetization decay, due to its collective nature, may not be, and indeed is expected not to be, monoexponential. Therefore, a theoretical model for the protein proton collective relaxation decays is needed before relaxation dispersion profiles can be obtained and interpreted.

A model for the collective relaxation of protein proton spins is here developed and validated with experimental measurements. The model is then used for a more quantitative analysis of the relaxation dispersion profiles. It is found that such analysis can provide direct information on an overall “collective” order parameter,¹⁶ on the reorientation correlation time of the protein, and thus on possible aggregation/oligomerization phenomena. The proteins selected for the study are two globular proteins:

- (1) Clore, G. M.; Szabo, A.; Bax, A.; Kay, L. E.; Driscoll, P. C.; Gronenborn, A. M. *J. Am. Chem. Soc.* **1990**, *112*, 4989–4991.
- (2) Mandel, A. M.; Akke, M.; Palmer, A. G., III. *J. Mol. Biol.* **1995**, *246*, 163.
- (3) Baber, J. L.; Szabo, A.; Tjandra, N. *J. Am. Chem. Soc.* **2001**, *123*, 3953–3959.
- (4) Halle, B.; Denisov, V. P. *Methods Enzymol.* **2001**, *338*, 178–201.
- (5) Butterwick, J. A.; Loria, J. P.; Astrof, N. S.; Kroenke, C. D.; Cole, R.; Rance, M.; Palmer, A. G., III. *J. Mol. Biol.* **2004**, *339*, 855–871.
- (6) Korzhnev, D. M.; Salvatella, X.; Vendruscolo, M.; Di Nardo, A. A.; Davidson, A. R.; Dobson, C. M.; Kay, L. E. *Nature* **2004**, *430*, 586–590.
- (7) Nusser, W.; Kimmich, R. *J. Phys. Chem.* **1990**, *94*, 5637–5639.
- (8) Korb, J.-P.; Bryant, R. G. *J. Chem. Phys.* **2001**, *115*, 10964–10974.
- (9) Bertini, I.; Gupta, Y. K.; Luchinat, C.; Parigi, G.; Schlörb, C.; Schwalbe, H. *Angew. Chem., Int. Ed.* **2005**, *44*, 2–4.
- (10) Rinck, P. A.; Fischer, H. W.; Vander Elst, L.; Van Haverbeke, Y.; Muller, R. N. *Radiology* **1988**, *168*, 843–849.

- (11) Koenig, S. H.; Brown, R. D., III. *Progr. NMR Spectrosc.* **1990**, *22*, 487–567.
- (12) Lopiano, L.; Fasano, M.; Giraud, S.; Digilio, G.; Koenig, S. H.; Torre, E.; Bergamasco, B.; Aime, S. *Neurochem. Int.* **2000**, *37*, 331–336.
- (13) Kimmich, R.; Anardo, E. *Progr. NMR Spectrosc.* **2004**, *44*, 257–320.
- (14) Kowalewski, J.; Maler, L. *Nuclear Spin Relaxation in Liquids: Theory, Experiments, and Applications*; Taylor & Francis: 2006; pp 1–440.
- (15) Ferrante, G.; Sykora, S. *Adv. Inorg. Chem.* **2005**, *57*, 405–470.
- (16) Lipari, G.; Szabo, A. *J. Am. Chem. Soc.* **1982**, *104*, 4546–4559.

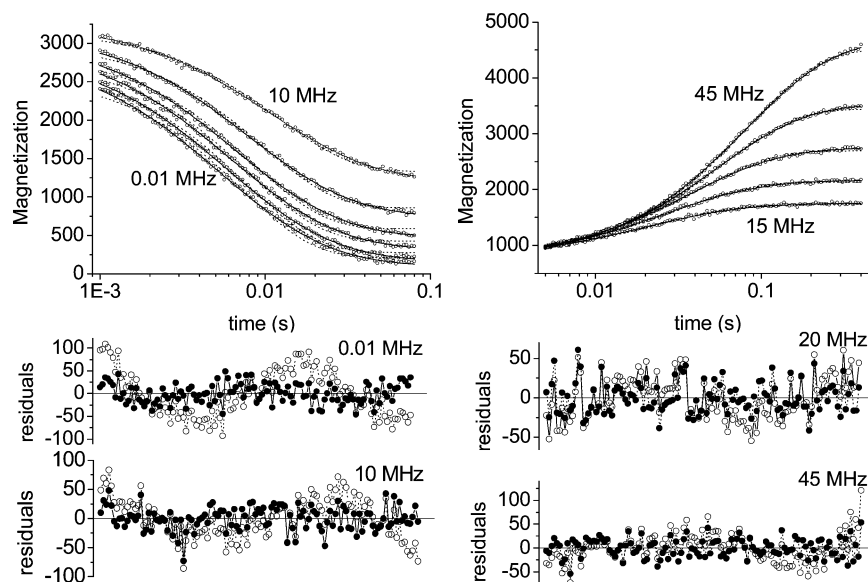


Figure 1. Magnetization decay/recovery for the HEWL sample at some magnetic fields (0.01, 0.85, 2.28, 3.73, 6.1, 10 MHz (panel on the left); 15, 20, 26, 34, 45 MHz (panel on the right)) and best fit lines calculated using the distribution of the relaxation rates reported in Figure 2C or the distribution of energies reported in Figure 2F (solid lines). The monoexponential fit is also shown as dotted lines. The residuals obtained when the fit is performed with the distribution of relaxation rates (solid symbols) are essentially unbiased, within the experimental scattering, whereas the residuals obtained with a monoexponential fit (open symbols) are clearly biased, especially at low field.

hen egg white lysozyme (HEWL, MW 16 kDa) and human serum albumin (HSA, MW 64 kDa).

Methods

HEWL and HSA (fatty acid free (~0.005%), essentially globulin free) were purchased from SIGMA (Milan, Italy) and used without further purification. The proteins were dissolved in 99.9% D₂O, lyophilized, and redissolved in D₂O three times, the last time in 99.996% D₂O. The final solution was under argon atmosphere to avoid dissolved oxygen. The sample volume was 0.5 mL. The concentrations were 2.8 and 0.94 mM for HEWL and HSA, respectively.

The longitudinal magnetization decay/recovery curves for the two proteins at 20 different magnetic field values in the range 0.01–45 MHz were measured using the standard field cycling technique with a Stellar Spinmaster FFC-2000-1T.¹⁵ The switching time, i.e., the time needed to change the field during the cycling, was set to the minimum allowed value, which is 0.0013 s for fields lower than 15 MHz (when a prepolarized sequence is used) and 0.005 s for higher fields. The NMR signal was time averaged (64 scans) and measured for 120 logarithmically spaced times from 0.001 to 0.08 s below 15 MHz, and up to 0.4 s above 15 MHz, for HEWL. For HSA, the NMR signal was measured from 0.001 s up to times for which the magnetization decay/recovery was essentially completed. The latter times ranged from 0.02 s at 0.01 MHz up to 2 s above 15 MHz. The polarization time was set to 0.2 s for HEWL and 1 s for HSA. The choice of these times permits us to drastically reduce the water proton contribution to relaxation rates. In any case, the latter could be easily separated from protein proton relaxation rates even for the HSA sample at large fields, due to the much longer relaxation time of water protons. The NMR signal from the protein protons showed signal-to-noise (*S/N*) ratios of about 50 on a 64 scan acquisition (detection field of 13 MHz, polarization field of 30 MHz).

The program OriginPro was used for the fit of the data.

Results

Modeling Collective Protein Proton Relaxation Rates.

Recently, a high sensitivity relaxometer has been developed.¹⁵ The sensitivity of such an instrument with respect to the older generations has increased to the point where the instrument is

now capable of detecting the signal of protein protons in millimolar protein solutions in D₂O with a good signal-to-noise ratio.⁹ The magnetization decay/recovery detected from relaxometric measurements is thus the sum of the magnetization decays/recoveries for all nonexchangeable protons in the protein solute. At this point, the physical significance of the collective behavior of the protein proton magnetization depends only on our ability to develop a suitable interpretive model.

The time dependence of the collective magnetization of protein protons in a 2.8 mM solution of lysozyme in D₂O at pH* 3.5 has been acquired for a wide range of magnetic fields, from 0.01 to 45 MHz of proton Larmor frequency. Low field data (up to 15 MHz) are acquired in the “prepolarized” mode; i.e., the data provide decay curves from the prepolarized intensity at 30 MHz to that at the relaxation field. Conversely, data above 15 MHz are acquired in the “direct” mode; i.e., they provide magnetization buildup curves from zero field to the relaxation field. The high quality of the data is immediately apparent from the small scatter of the data points along each decay/recovery curve (Figure 1). It is also apparent that such curves cannot be satisfactorily fit by a monoexponential function (dotted lines in Figure 1). This was expected, since different protein protons have different relaxation rates, depending on the energy of the dipolar interactions with neighboring protons. The fits performed with a biexponential function are instead excellent. Interestingly, at all fields the weight of the first exponential function was about 67% of the total, and the rate of the second exponential function was about a factor of 4 larger than the rate of the former. This experimental evidence suggests that the underlying model should be rather simple.

In theory, each protein proton has its own relaxation rate. For a given protein of known structure, and neglecting all kinds of internal motions, such rates can be predicted by using a relaxation matrix approach, for instance using the program CORMA.^{17,18} We have therefore simulated with CORMA the

(17) Keepers, J. W.; James, T. L. *J. Magn. Reson.* **1984**, *57*, 404–426.

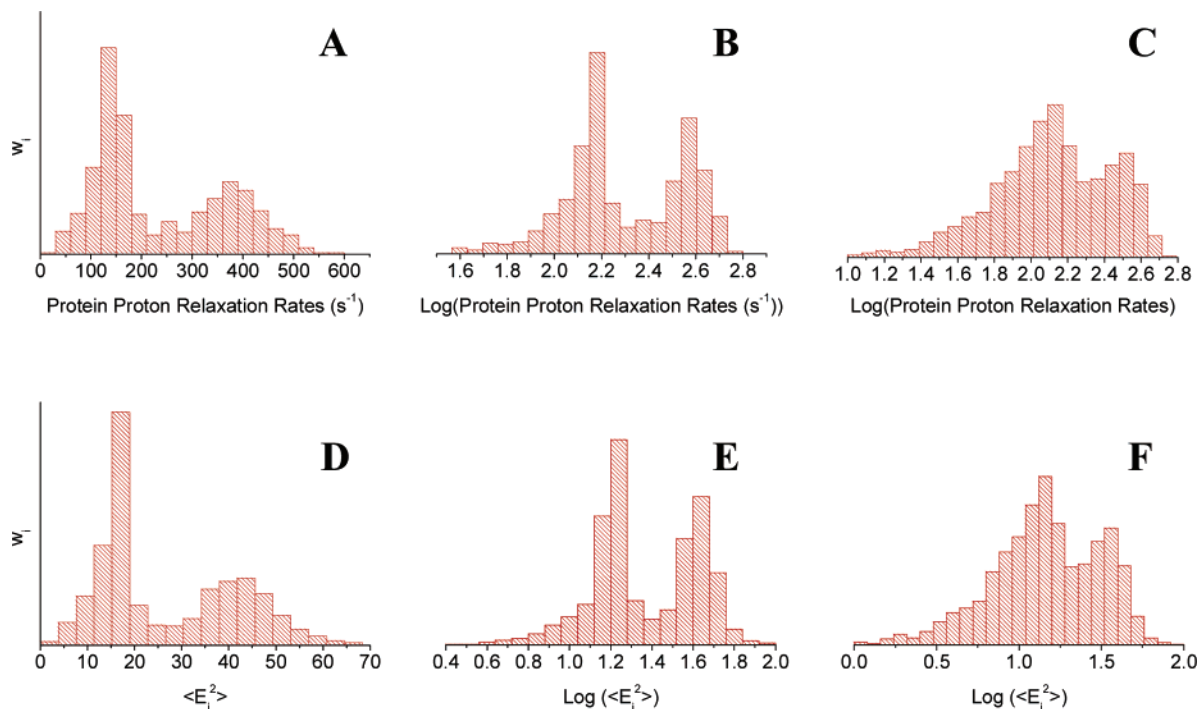


Figure 2. Relaxation rate distribution as calculated with CORMA at low fields for HEWL on a linear (A) and a logarithmic (B) scale. Methyl proton relaxation rates have been multiplied by 0.25 to account for rotation. Panel C shows the logarithmic distribution after S^2 -spreading. The average “universal” mean squared dipolar energy distribution calculated with CORMA for the 20 well-folded proteins is reported on a linear (D) and a logarithmic (E) scale. Panel F shows the average “universal” mean squared dipolar energy distribution on a logarithmic scale after S^2 -spreading. The distribution in panel F is the one used to fit the magnetization decays/recoveries (reported in Figure 1 as solid lines). The ratios of the $\langle E_i^2 \rangle$ values with respect to the $\langle E_i^2 \rangle$ value of the highest peak and the relative weights \bar{w}_i (in parentheses) are as follows: 0.11 (0.0076), 0.13 (0.0079), 0.16 (0.0051), 0.19 (0.0098), 0.229 (0.0166), 0.275 (0.0234), 0.331 (0.0267), 0.398 (0.0316), 0.479 (0.0532), 0.575 (0.0673), 0.692 (0.0784), 0.832 (0.102), 1.0 (0.1223), 1.202 (0.0881), 1.445 (0.0566), 1.74 (0.0588), 2.09 (0.0751), 2.512 (0.0849), 3.02 (0.0575), 3.63 (0.0208), 4.37 (0.0069). The $\langle E_i^2 \rangle$ values are expressed in 10^9 s^{-2} .

detailed relaxation behavior of all protein protons in HEWL at 298 K under nonselective excitation conditions, such as those operative in relaxometric measurements. The rotational correlation time was estimated through the program HYDRONMR.¹⁹ By considering the 25% increase in viscosity of D_2O with respect to H_2O ,²⁰ the obtained value was 9 ns. The three-dimensional structure of the protein was taken from the PDB files 1DPX and 4LZT.

First of all, we find that the magnetization decay calculated by CORMA for each nonexchangeable proton signal (nonexchangeable protons are here defined as all the CH, CH_2 , and CH_3 protons and HN in helical or β -sheet secondary structures²¹) at low field can be fit to a very good precision by a monoexponential function, and an individual relaxation rate can thus be calculated (in fact, although the magnetization decay is provided by the sum of the exponential decays with time constants given by the eigenvalues of the relaxation matrix and weighted by the eigenvectors, in practice at low field one coefficient is much larger than all others). Therefore, at low field, a distribution of relaxation rates can be obtained, and the time dependence of the overall magnetization can be predicted and compared with the experimental one. At higher field the situation is more complex, because spin diffusion begins to be

operative. Under these conditions *nonexponential* behavior is expected and observed, with protons relaxing slowly increasing, and protons relaxing rapidly decreasing, their decay/recovery rate with time. However, as the ensemble of protons in a protein in D_2O is effectively a closed spin system, the sum of all magnetization decays/recoveries is still effectively reproduced by a multiexponential behavior, as can be easily verified by appropriate CORMA calculations.

However, while the relaxation behavior of CH, CH_2 , and NH protons is presumably already well predicted by CORMA, that of methyl protons needs to be adapted to accommodate for the fast jump of methyl protons from one potential well to another along their rotation about the methyl group ternary axis.^{22,23} In fact, such rotation produces an averaging of the intra-methyl proton–proton dipolar relaxation resulting in a squared order parameter^{16,23} (S_{int}^2) of 0.25, as can be calculated by assuming the proton–proton vector to be at 90° with respect to the rotation axis.²⁴ Therefore, the relaxation rate values calculated by CORMA for methyl protons at low fields must be multiplied by 0.25.

The distribution of relaxation rates at low fields so calculated is reported in Figure 2A. Interestingly the distribution of relaxation rates spans over a range larger than a factor 5, and it is bimodal, the relaxation rate of the second peak being about 3 times larger than the relaxation rate of the first peak. The

(18) Borgias, B.; Gochin, M.; Kerwood, D. J.; James, T. L. *Progr. NMR Spectrosc.* **1990**, *22*, 83–100.

(19) García de la Torre, J.; Huertas, M. L.; Carrasco, B. *J. Magn. Reson.* **2000**, *147*, 138–146.

(20) Weast, R. C. *Handbook of Chemistry and Physics*; CRC Press: Boca Raton, FL, 1986.

(21) Banci, L.; Benedetto, M.; Bertini, I.; Del Conte, R.; Piccioli, M.; Richert, T.; Viezzoli, M. S. *Magn. Reson. Chem.* **1997**, *35*, 845–853.

(22) Tropp, J. *J. Chem. Phys.* **1980**, *72*, 6035–6043.

(23) Sherry, A. D.; Keepers, J.; James, T. L.; Teherani, J. *Biochemistry* **1984**, *23*, 3181–3185.

(24) Woessner, D. E. *J. Chem. Phys.* **1962**, *36*, 1–4.

first peak mostly corresponds to the relaxation rates of CH, nonexchangeable NH, and methyl protons. The second peak corresponds to CH₂ protons. The relative amplitude of the two peaks is about 0.6:0.4.

The calculated distribution of protein proton relaxation rates should be directly usable to fit the experimental collective magnetization decays. Each collective magnetization decay at any field would thus be given by the sum of several exponential decays with different weights w_i and rates R_i , according to the distribution reported in Figure 2A. Since the experimental data have been acquired on an equally sampled logarithmic scale, a more correct distribution would be on a logarithmic scale, as shown in Figure 2B.

A fit was thus attempted using as a fit parameter one relaxation rate value, R_A , and fixing w_i and all the R_i/R_A ratios according to the calculated distribution (Table 1). The fit, although much better than that obtained with a monoexponential decay, is however unsatisfactory, because it is still significantly worse than that obtained with a simple biexponential decay. Moreover, the best fit relaxation rates are significantly smaller than those in the distribution calculated with CORMA in the assumption of rigid protein structures. This is due to the presence of internal local motions, which are fast on the reorientational time scale of the protein and decrease the relaxation rate of the protein protons at low field. Such a decrease is actually proportional to the extent of the motion to which each protein proton is subjected or, in other words, to its local S^2 value. As a consequence, the relaxation rate distribution was modified by introducing a distribution of S^2 values for each rate in the original distribution. The weight w_j for each S^2 value was assumed to be in simple direct linear dependence with the S^2 value itself ($w_j = S^2$). Therefore, each rate R_i was split into 10 rates given by $S_j^2 R_i$ with S_j^2 spanning from 0.1 to 1 in steps of 0.1, and with weights S_j^2 . The new weights for the rates R_i thus resulted in the \bar{w}_i :

$$\bar{w}_i = \frac{w_i \sum_j w_j S_j^2}{\sum_j w_j} = \frac{w_i \sum_j S_j^4}{\sum_j S_j^2} \quad (1)$$

The new distribution, clearly more spread, is reported in Figure 2C. The relative amplitude of the two peaks is now about 0.7:0.3, and the average relaxation rate of protons in the first peak is about 3.5 times larger than the average relaxation rate of protons in the second peak. These features explain why the fits obtained with a simple biexponential function, where the two exponentials were in a $2^{1/3}:1/3$ ratio and differed by a factor of approximately 4, were so satisfactory.

Such a simple model is supported by literature data on the distribution of S^2 values in proteins^{25–28} and was confirmed by a sample calculation of the autocorrelation function of the interacting nuclear vectors, according to Lipari and Szabo,¹⁶ where also the distance changes were considered. This calcula-

Table 1. Glossary of the Symbols Used and Their Physical Meaning in This Work

$J(\omega, \tau)$	spectral density, a function of the nuclear Larmor frequency $\omega/2\pi$ and of a correlation time τ
$M(t)$	collective magnetization of protein protons (defined as the sum of the magnetization of all individual protein protons) as a function of time
R_1	collective protein proton relaxation rate (defined as the average of the relaxation rates of individual protons)
R_i	any protein proton relaxation rate within the obtained distribution of values
R_A	a fixed value of the protein proton relaxation rate within the distribution
w_i	weight of the i th protein proton relaxation rate, R_i , as calculated with CORMA in the absence of internal motions
\bar{w}_i	weight of the i th protein proton relaxation rate, R_i , as calculated considering the presence of internal motions
S^2	squared order parameter as defined in the standard Lipari–Szabo model free approach ¹⁶
S_C^2	collective squared order parameter
ϵ	shrink factor introduced to mimic the effect of spin-diffusion
$\langle E_i^2 \rangle$	mean squared dipolar interaction energy of the i th protein proton with its neighbors
$\langle E^2 \rangle$	average of the mean squared dipolar interaction energies, $\langle E_i^2 \rangle$, of all protein protons
τ_R	protein reorientational time
$\langle \tau_i \rangle$	average correlation time for fast protein proton internal motions

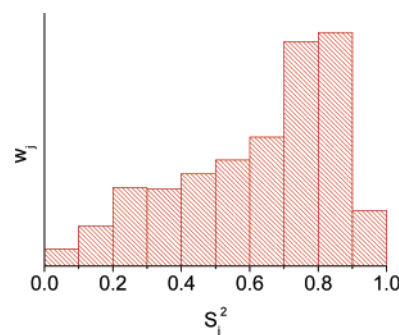


Figure 3. Distribution of the S^2 values calculated from a molecular dynamics calculation²⁹ on the C2 domain of the protein kinase C β for all dipolar interactions of each non-methyl proton with its closest protein proton.

tion was performed using a 1.6 ns molecular dynamics simulation on the C2 domain of the protein kinase C β .²⁹ The obtained S^2 distribution for all interactions involving all NH, CH, and methylene protons with the closest proton is reported in Figure 3. S^2 for methyl protons is calculated to be up to 0.25, as expected.

Furthermore, CORMA calculations performed in the assumption of rigid protein structures indicate that the ratio between the relaxation rates at the two peaks is constant up to 10 MHz and starts slightly to decrease and approach 1 for larger frequencies in the case of HEWL, i.e., for a protein with a reorientational time of 9 ns. For more slowly rotating proteins, such a ratio starts to decrease at earlier frequencies. This behavior is expected and is due to spin-diffusion effects that become operative at proton Larmor frequencies larger than the reciprocal of the rotational correlation time. They thus become

(25) Case, D. A. NMR Refinement; In *Encyclopedia of Computational Chemistry*; J. Wiley & Sons: 1998.

(26) Chou, J. J.; Case, D. A.; Bax, A. *J. Am. Chem. Soc.* **2003**, *125*, 8959–8966.

(27) Buck, M.; Boyd, J.; Redfield, C.; MacKenzie, D. A.; Jeenes, D. J.; Archer, D. B.; Dobson, C. M. *Biochemistry* **1995**, *34*, 4041–4055.

(28) Ming, D.; Brüschweiler, R. *J. Biomol. NMR* **2004**, *29*, 363–368.

(29) Banci, L.; Cavallaro, G.; Kheifets, V.; Mochly-Rosen, D. *J. Biol. Chem.* **2002**, *277*, 12988–12997.

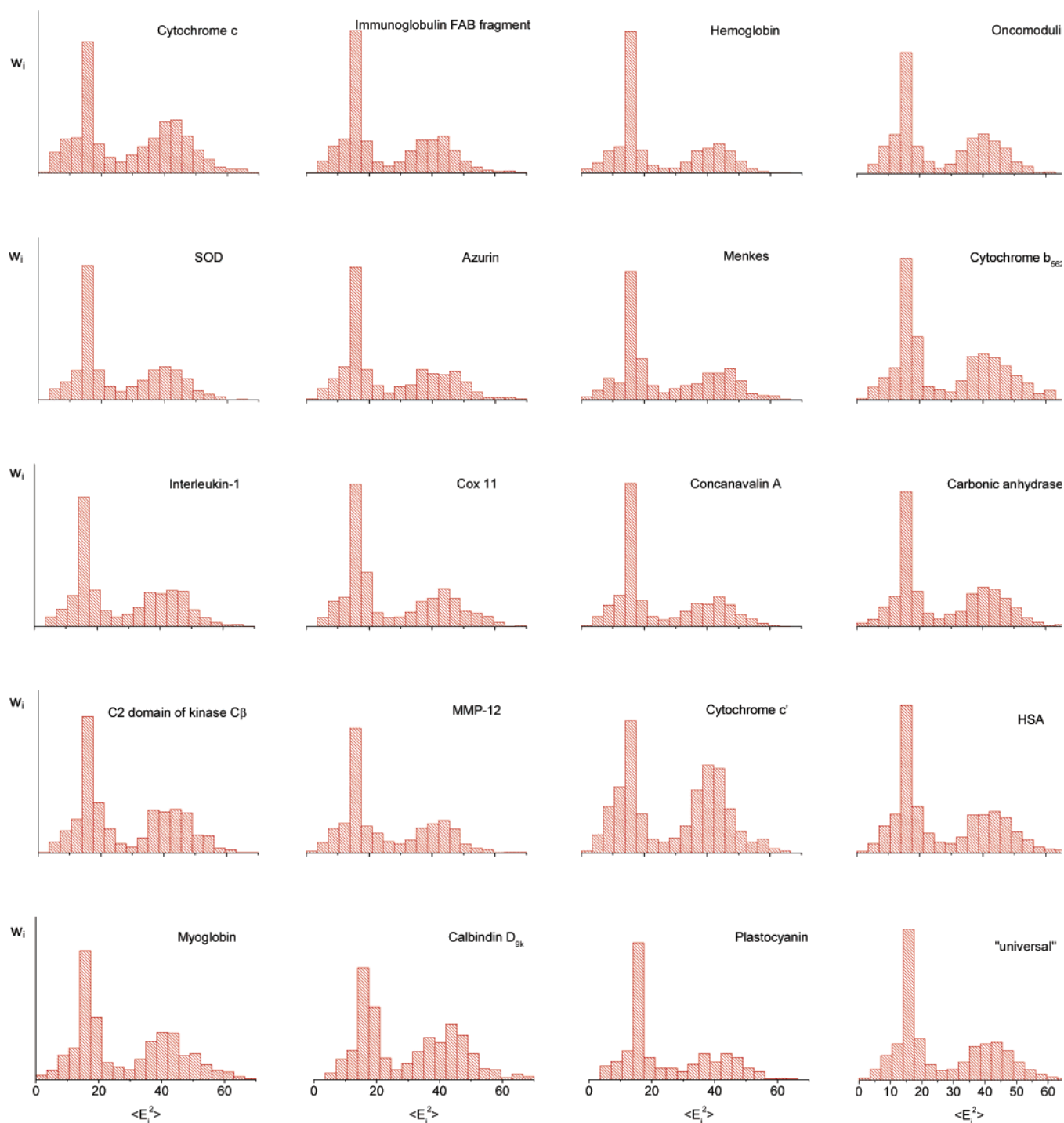


Figure 4. Relaxation rate distributions on a linear scale calculated with CORMA at low fields for several proteins, normalized to the protein reorientational time ($\langle E_i^2 \rangle$, expressed in 10^9 s^{-2}). The “universal” distribution is also shown.

important at increasingly low frequencies as the rotational correlation time of the protein increases. In order to mimic this effect a shrink parameter, ϵ , was introduced. The collective protein proton relaxation rates were thus modeled according to the equation

$$R_1(\omega) = \sum_i \bar{w}_i R_A (R_i/R_A)^{1+\epsilon} \quad (2)$$

which at low fields reduces to $R_1(0) = \sum_i \bar{w}_i R_i$. The fourth ϵ

parameter is in fact expected to assume values that are different from zero and negative only when spin diffusion becomes operative, i.e., at relatively high fields. This is indeed observed (see below). At each magnetic field, the magnetization decay/recovery was thus fit according to the equations

$$M(t) = \beta \sum_i \bar{w}_i \exp[-R_A (R_i/R_A)^{1+\epsilon} t] + \gamma$$

$$M(t) = \beta \sum_i \bar{w}_i \{1 - \exp[-R_A (R_i/R_A)^{1+\epsilon} t]\} + \gamma \quad (3)$$

containing four fit parameters: the relaxation rate corresponding, e.g., to the first peak of the distribution, R_A , ϵ , β , and γ .

The fits of the magnetization decays/recoveries of HEWL for different magnetic fields according to eq 3 and the distribution of rates reported in Figure 2C are all excellent (Figure 1). The fits provided shrink factors ϵ about constant and close to zero (± 0.1) for all magnetization decays below 25 MHz, while increasingly negative values of ϵ are obtained for larger fields, the smallest value resulting in -0.33 at 45 MHz. Such shrinking in the distribution of relaxation rates is indeed confirmed by performing CORMA calculations at high fields (see Supporting Information). The collective protein proton relaxation rates thus calculated (eq 2) are reported in Figure 5 as a function of field.

Generality of the Model. We show here that the model that we propose is of general validity. We calculated the distribution of relaxation rates at low field for a series of protein structures with size spanning from 75 to 600 residues (cytochrome b_{562} , cytochrome c , cytochrome c' , myoglobin, interleukin-1 beta, immunoglobulin FAB fragment, plastocyanin, azurin, concanavalin A, carbonic anhydrase II, hemoglobin, superoxide dismutase, matrix metalloproteinase-12 catalytic domain, calbindin D_{9k} , menkes, cox 11, oncomodulin, C2 domain of kinase $C\beta$, lysozyme, human serum albumin), some solved by NMR, and some by X-ray, some all alpha, some all beta, and some alpha+beta proteins. These distributions, normalized to the τ_R values of each protein, are reported in Figure 4, and they clearly appear very similar. At low field, the normalized R values (R/τ_R) represent a measure of the mean squared energy related to the dipolar interactions for each proton, $\langle E_i^2 \rangle$. Their weighted average values,

$$\langle E^2 \rangle = \sum_i w_i \langle E_i^2 \rangle \quad (4)$$

can also be defined as the average mean squared dipolar interaction energies within each protein. The $\langle E^2 \rangle$ values result in being almost constant and equal to $(27 \pm 3) \times 10^9 \text{ s}^{-2}$ for all investigated proteins. An average “universal” mean squared dipolar energy distribution can be thus defined, and it is reported in Figure 2D. As discussed in the preceding section, the presence of internal motions again results in a spreading of the plots in Figures 2D,E and 4, as shown in Figure 2F. This average distribution is characterized by the weights \bar{w}_i and the squared dipolar energy ratios R_i/R_A reported in the caption to Figure 2. Both values are very close to the values calculated specifically for lysozyme. When this model is used to fit experimental magnetization decays of lysozyme, the resulting fit is very similar to that obtained using the specific lysozyme distribution, providing $R_1(\omega)$ values within 1% of the previous ones (Figure 5). This model for the protein proton relaxation rate distribution can be applied to all globular proteins without further calculations.

The theoretical analysis of the distribution of the relaxation rates, experimentally confirmed by measurements on HEWL, brings the following conclusions: (i) the high quality of the magnetization recovery/decay allows us to safely pinpoint a multiexponential behavior; (ii) the whole set of field dependent data can be fit with a modeled relaxation rate distribution that originates from a complete relaxation matrix analysis and takes into account a realistic distribution of local S^2 values; (iii) the

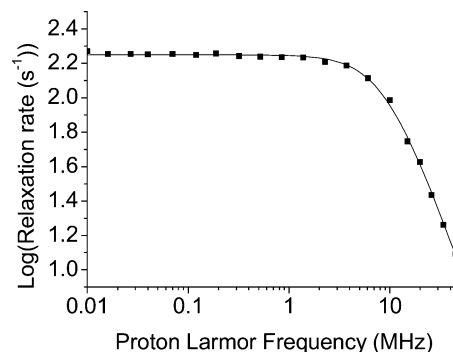


Figure 5. Collective protein proton relaxation rates for a 2.8 mM HEWL solution in D_2O . The solid line shows the best-fit profile according to eq 8.

modeled relaxation rate distribution can be obtained for any protein of known structure; (iv) the modeled relaxation rate distributions calculated for a large number of proteins of known structure are very similar, allowing us to define a “universal” distribution whose low field average rate shows a spreading of about $\pm 10\%$; (v) such a “universal” distribution can be used, to a good approximation, to fit the data even when the protein structure is unknown.

Generating Collective Protein Proton Relaxation Dispersions from Experimental Data. By using the model described and validated in the previous section, the collective protein proton relaxation rates can be reliably extracted from the acquired protein proton magnetization recovery/decays at all fields. Once these rates are obtained from the data, their dependence on the magnetic field contains relevant dynamic information on the system under investigation that in turn needs to be extracted.

The collective protein proton relaxation rates, R_1 , must be related to the spectral density function $J(\omega, \tau)$ through the mean squared dipolar interaction energy, $\langle E^2 \rangle$ defined in eq 4:

$$R_1 = S_C^2 \langle E^2 \rangle J(\omega, \tau_R) + (1 - S_C^2) \langle E^2 \rangle J(\omega, \tau_f) \quad (5)$$

This equation takes into account the fact that all protein protons are subjected to additional local fast motions, besides the global reorientational time, as already anticipated in the preceding sections, using the Lipari–Szabo formalism.¹⁶ Fast motions are parametrized through a term S_C^2 , which is expected to vary from one protein to another depending on their degree of rigidity. S_C^2 thus represents a “collective” order parameter needed to match the collective relaxation rates obtained from the fit of the experimental magnetization decays, which are sensitive to the S^2 value of individual proton pairs (see eq 2), with the relaxation rates calculated with CORMA in the assumption of rigid structures. τ_R and τ_f are the relevant parameters to extract dynamic information; τ_R is the reorientation time of the protein, and τ_f is the correlation time for local motions. It should be noted that in the preceding sections we have incorporated only the effect of the *spreading* of the local S^2 values in the calculated average relaxation rate distribution. The actual overall reduction of the average relaxation rate due to these local S^2 values is entirely described by the S_C^2 parameter introduced here.

The form of $J(\omega, \tau)$ to be used to fit the collective protein proton relaxation dispersion is not obvious to determine, as methyl protons should behave as like spins, while CH protons at low fields should behave as unlike spins and methylene

Table 2. Best-Fit and Theoretical Parameters for HEWL 2.8 mM (pH* 3.5) and HSA 0.94 mM and 1.8 mM (pH* 7.4) at 298 K in Deuterated Water

	calculated τ_R (10^{-9} s)	experimental τ_R (10^{-9} s)	calculated $\langle E^2 \rangle$ (10^9 s $^{-2}$)	S_C^2	α (s $^{-1}$)	χ^2
HEWL	9.0 ^{a,b}	9.0 ± 0.2	25.87 ^a	0.75 ± 0.02	2.2 ± 0.6	0.000 19
HSA 0.94 mM	57.5 ^b	66 ± 2	28.33	0.81 ± 0.02	3.3 ± 0.2	0.000 68
	63 ^c	63 (92%), 126 (8%) ^d		0.80 ± 0.02	3.3 ± 0.2	0.000 50
HSA 1.8 mM	57.5 ^b	94 ± 3	28.33	0.73 ± 0.03	2.6 ± 0.3	0.001 06
	72 ^c	72 (64%), 144 (36%) ^d		0.72 ± 0.02	2.5 ± 0.2	0.000 51

^a Values calculated from the PDB structure 4LZT (0.95 Å resolution). Values of 9.1×10^{-9} s and 26.10×10^9 s $^{-2}$ can be calculated for the theoretical τ_R and $\langle E^2 \rangle$ values, respectively, from the PDB structure 1DPX (1.65 Å resolution). ^b Calculated with HYDRONMR. ^c HYDRONMR value corrected using eq 9. ^d Imposed τ_R values for monomers and dimers, with the best fit % contribution of each in parentheses.

protons could effectively behave as like spins although they are strictly speaking unlike spins, in a chiral environment such as a protein. The two $J(\omega, \tau)$ functions commonly used for like and unlike spins are given by eqs 6 and 7, respectively:

$$J_1(\omega, \tau) = \frac{0.8\tau}{1 + 4\omega^2\tau^2} + \frac{0.2\tau}{1 + \omega^2\tau^2} \quad (6)$$

$$J_2(\omega, \tau) = \frac{0.6\tau}{1 + 4\omega^2\tau^2} + \frac{0.3\tau}{1 + \omega^2\tau^2} + 0.1\tau \quad (7)$$

Due to cross relaxation/spin diffusion effects that become operative at higher fields, both forms of $J(\omega, \tau)$ could in principle be inappropriate. We have thus calculated the collective protein proton relaxation rate through CORMA from very low to very high magnetic fields and fitted the resulting dispersion at each field. The fit performed with either eq 6 or 7, as well as a combination of the two (see Supporting Information), clearly indicated that eq 6 should be used, as it is in perfect agreement with the simulated data and able to provide as best fit parameters the very same input values of $\langle E^2 \rangle$ and τ_R provided in the simulation. Note that it is only the collective protein proton relaxation rate dispersion that is fit perfectly by eq 6. If dispersions for individual protons are calculated, they all deviate sensibly from either eq 6 or 7 or any combination thereof, due to the onset of cross relaxation/spin diffusion effects at high field (see Figure S2), as already noted. This is discussed in more detail in the Supporting Information.

The equation used to fit the experimental relaxation dispersion profiles is thus⁹

$$R_1 = S_C^2 \langle E^2 \rangle \left(\frac{0.8\tau_R}{1 + 4\omega^2\tau_R^2} + \frac{0.2\tau_R}{1 + \omega^2\tau_R^2} \right) + \alpha \quad (8)$$

For a protein of known structure, the effective $\langle E^2 \rangle$ can be calculated with CORMA, τ_R and S_C^2 are the fit parameters discussed above, and α is the high field limit for relaxation that incorporates the $(1 - S_C^2)\langle E^2 \rangle \langle \tau_f \rangle$ contribution in eq 5.

It should be noted that, in the present direct detection of protein proton signals, the nondispersive α term is not affected by the presence of water protons. Therefore, it precisely represents only the small $(1 - S_C^2)\langle E^2 \rangle \langle \tau_f \rangle$ contribution, as its dispersion is related to local motions occurring at time scales faster than those observable in the detected field range. This term can provide important information on the averaged correlation time for fast local motions, $\langle \tau_f \rangle$, which are not easily available from standard bulk water proton relaxation dispersion profiles. In fact, in the latter profiles, α also contains the

contribution from water protons exchanging faster than the protein reorientation time.

It should be noted that the τ_R value in eq 5 is exactly the reorientation time of the protein, at variance with the τ value that can be extracted from the bulk water ^2H and ^{17}O relaxation dispersions^{30–39} which is influenced by both the reorientational correlation time of the hydrated protein and by the lifetime of the weakly interacting waters. In water ^1H relaxation dispersions, also the lifetimes of exchangeable protein protons contribute to determine the position of the dispersion.^{40–44} Therefore, the estimation of the reorientational correlation time that can be obtained from direct protein proton relaxation rate dispersions is more accurate and straightforward.

Extracting Dynamic Information from the Relaxation Dispersion Profiles. The collective protein proton relaxation dispersion profile of 2.8 mM HEWL, shown in Figure 5, was then fit to eq 8. Since relaxation rate measurements are affected by similar percent errors (and not by similar absolute errors), a fit of the logarithms of the collective relaxation rate values was performed. The fits turned out to be excellent (Figure 5).

The obtained S_C^2 , α , and τ_R parameters are reported in Table 2 together with the theoretical predictions. The overall agreement of the present analysis of the experimental data with theoretical expectations fully validates the theoretical model developed here. From the best-fit parameters it appears that HEWL at pH* 3.5 is a monomeric rigid globular protein, with a τ_R of 9.0 ns, in accordance with the theoretical estimate and with previous measurements.^{27,44} The fit yields a collective S_C^2 of 0.75. The fit performed using the “universal” relaxation rate distribution (Figure 2F), instead of that calculated from the protein structure (Figure 2C), provided basically coincident best fit τ_R and S_C^2

- (30) Wiesner, S.; Kurian, E.; Prendergast, F. G.; Halle, B. *J. Mol. Biol.* **1999**, *286*, 233–246.
- (31) Van-Quynh, A.; Willson, S.; Bryant, R. G. *Biophys. J.* **2003**, *84*, 558–563.
- (32) Halle, B.; Davidovic, M. *Proc. Natl. Acad. Sci. U.S.A.* **2003**, *100*, 12135–12140.
- (33) Denisov, V. P.; Halle, B. *Biochemistry* **1998**, *34*, 9046–9051.
- (34) Denisov, V. P.; Jonsson, B.-H.; Halle, B. *Nat. Struct. Biol.* **1999**, *6*, 253–260.
- (35) Kumar, S.; Modig, K.; Halle, B. *Biochemistry* **2003**, *42*, 13708–13716.
- (36) Modig, K.; Kurian, E.; Prendergast, F. G.; Halle, B. *Protein Sci.* **2003**, *12*, 2768–2781.
- (37) Denisov, V. P.; Halle, B. *Faraday Discuss.* **1996**, *103*, 227–244.
- (38) Modig, K.; Liepinsh, E.; Otting, G.; Halle, B. *J. Am. Chem. Soc.* **2004**, *126*, 102–114.
- (39) Denisov, V. P.; Jonsson, B.-H.; Halle, B. *J. Am. Chem. Soc.* **1999**, *121*, 2327–2328.
- (40) Libralleso, E.; Nerinovski, K.; Parigi, G.; Turano, P. *Biochem. Biophys. Res. Commun.* **2005**, *328*, 633–639.
- (41) Kiihne, S.; Bryant, R. G. *Biophys. J.* **2000**, *78*, 2163–2169.
- (42) Venu, K.; Denisov, V. P.; Halle, B. *J. Am. Chem. Soc.* **1997**, *119*, 3122–3134.
- (43) Banci, L.; Berners-Price, S.; Bertini, I.; Clementi, V.; Luchinat, C.; Spyroulias, G. A.; Turano, P. *Mol. Phys.* **1998**, *95*, 797–808.
- (44) Gottschalk, M.; Halle, B. *J. Phys. Chem. B* **2003**, *107*, 7914–7922.

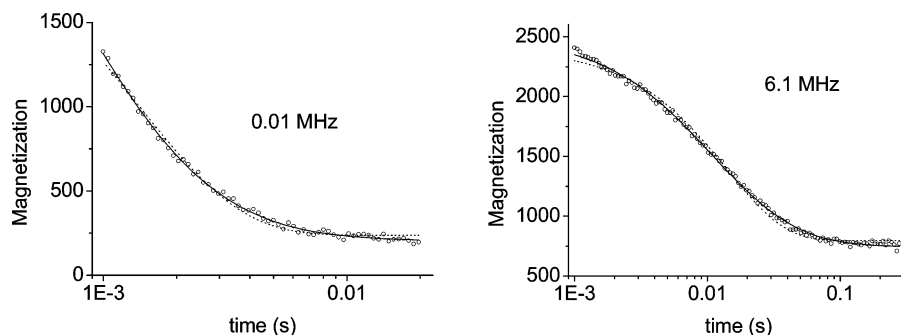


Figure 6. Magnetization decay for the 0.94 mM HSA sample at a 0.01 and 6.1 MHz proton Larmor frequency and best fit lines calculated using the distribution of the relaxation rates (solid lines). The monoexponential fits are also shown as dotted lines.

values. The latter result demonstrates the possibility of obtaining information also from proteins of unknown structure.

HSA: Analysis of the Experimental Data in the Light of the Model. Collective protein proton magnetization decays were acquired also for solutions of HSA in D₂O. The experimental data were analyzed as done for the previously reported lysozyme data. The squared dipolar energy distribution was first calculated from the PDB structure 1BM0, as reported in Figure 4.

Being a protein of four times the size of lysozyme, HSA is expected to yield collective relaxation rates at low field larger than 10^3 s^{-1} . At present, the time needed to cycle from the relaxation field to the measuring field is of the order of a millisecond, implying that signals with R_1 higher than about 10^3 s^{-1} are largely lost. Actually, the presence of the higher relaxation components could not be obtained from the low field experimental data but predicted from the magnetization decay at higher fields and the imposition of the calculated relaxation rate distribution. As a consequence, a fit of the magnetization decay performed without knowledge of the relaxation rate distribution would have proven particularly incorrect in this case. In fact, if the protein magnetization has a multiexponential decay, then a sizable loss of the faster relaxing components alters the ratio of the components in the distribution, and the fit is biased toward the slower relaxing components. Furthermore, an additional exponential decay due to the residual water proton relaxation rate was introduced, as the required longer polarization time makes the residual water proton magnetization not negligible anymore. Such decay was estimated to be about 0.3 s^{-1} . In fact, whereas the free water proton relaxation rate is negligibly small in highly deuterated solutions (less than 0.05 s^{-1}),⁴⁵ residual water proton relaxation due to the interaction with the protein is about $0.2\text{--}0.3 \text{ s}^{-1} \text{ mM}^{-1}$ in HSA solutions.^{41,46}

The fit of the collective protein proton magnetization decay/recovery to the modeled distribution for a 0.94 mM HSA solution is good (see Figure 6), while also in this case the fit performed using a monoexponential decay function is not satisfactory. The resulting collective relaxation rate dispersions are reported in Figure 7, together with the best fit profile performed according to eq 8. The reorientational time estimated for HSA through HYDRONMR was 58 ns. However, the fit provided a correlation time of $66 \pm 2 \text{ ns}$, somewhat higher than the theoretical estimate. Such a discrepancy is not dramatic but,

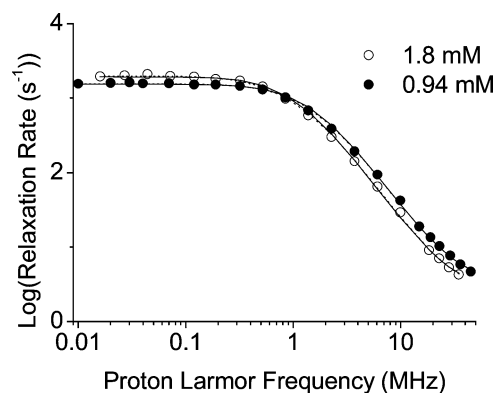


Figure 7. Collective protein proton relaxation rates for HSA 0.94 mM (solid symbols) and 1.8 mM (open symbols). The solid lines show the best-fit profiles obtained with the assumption of a single reorientational time. The dotted line shows the fit calculated in the presence of both monomer and dimeric species.

given the accuracy of the estimate of τ_R provided by the present approach, should reflect a real physical phenomenon. One possibility is an increase of the viscosity of the HSA solution with respect to that of the solvent. It is known that the microscopic viscosity, i.e., the viscosity sensed by the solute itself, does not increase with the amount of dissolved solute (while the macroscopic viscosity does). However, this holds until the fractional volume occupied by the solute is negligibly small compared to the volume of the solution. Actually, a 0.94 mM solution of HSA (MW 64 000) has already a larger fractional volume than the 2.4 mM solution of HEWL (MW 16 000). Empirical equations for the microscopic viscosity (η_{mic}) when the fractional solute volume is not negligible have been proposed. For example, the following equation

$$\frac{\eta_{mic} - \eta_0}{\eta_0} = \frac{[(r/d)/(1 - r/d)]^3}{1 - [(r/d)/(1 - r/d)]^3} \quad (9)$$

has been found to agree with experimental water proton relaxation data in protein solutions¹¹ (r is the protein radius, and d is the average interprotein separation). According to eq 9, an increase of viscosity of 9% is predicted for the present HSA solution, which translated into a τ_R value of 63 ns, i.e., intermediate between the observed value and that predicted by HYDRONMR. To obtain further information, the NMRD measurements were repeated on an even more concentrated solution (1.8 mM). In this case, a much higher τ_R value of $94 \pm 3 \text{ ns}$ was obtained. This value should be compared with the value of 72 ns predicted by eq 9 at this concentration, which

(45) Koenig, S. H.; Bryant, R. G.; Hallenga, K.; Jacob, G. S. *Biochemistry* **1978**, *17*, 4348–4358.

(46) Bertini, I.; Fragai, M.; Luchinat, C.; Parigi, G. *Magn. Reson. Chem.* **2000**, *38*, 543–550.

yields an increase in viscosity of 25%. Therefore, the increase in microscopic viscosity explains only in part the increase in τ_R value observed for millimolar HSA solutions.

Another possibility is the presence of specific protein–protein interactions that lead to the partial formation of dimers, i.e., of species with a doubled value of τ_R , or even larger aggregates. In the presence of a fast exchange equilibrium between monomers and dimers,⁴⁷ which is a reasonable assumption in this case, the measured collective protein proton relaxation rate is in fact given by the weighted average between the rates calculated using eq 8 for the different reorientation times (for systems in slow exchange, such rates should instead be the constants of the double exponential time decay⁴⁷ of each proton magnetization). The profiles of the HSA solutions at the two concentrations were therefore fit by imposing the presence of monomers and dimers, with the τ_R values estimated from eq 9 (i.e., of 63 and 126 ns for monomers and dimers, respectively, at 0.94 mM, and of 72 and 144 ns for monomers and dimers, respectively, at 1.8 mM), and by letting only the ratio between the two forms free to vary. At variance with the HEWL case, the quality of the fit of relaxation rates actually improved by considering two dispersions (see χ^2 values in Table 2). The overall fit indicated a composition of about 92% monomer for the 0.94 mM solution and of about 64% monomer for the 1.8 mM solution. From these values a dimerization constant of about 10^2 M^{-1} can be obtained. It should be noted that the S_C^2 values obtained from the fit of the HSA solutions at the two concentrations are considerably different, while aggregation is not expected to influence much the internal mobility. As already stated, HSA shows high relaxation rates, which are at the limit of the present version of the instrument. A non-negligible fraction of the high end of the relaxation rate distribution may be lost, especially in the more concentrated sample. In turn, this would result in a lower average relaxation rate and therefore in an apparent lower S_C^2 value.

A Critical Assessment of the Reliability of the Fitting Parameters. The availability of the collective protein proton relaxation rates as a function of the field from very low magnetic fields up to 1 T directly permits an accurate and reliable determination of the reorientational time of the investigated proteins from the position of the relaxation dispersion. The accuracy of the τ_R value so obtained is larger with respect to that obtained with water proton relaxation measurements due to the contribution of exchanging protein protons and of water protons interacting with the protein, which affect the acquired water proton relaxation rates and are difficult to quantify.⁴⁰ High resolution measurements, on the other hand, can provide estimates of τ_R provided that the protein assignment is known and accurate T_1 , T_2 , NOE measurements are carefully analyzed with complete model-free treatments.⁴⁸ The method proposed here, on the contrary, can be applied to any protein, independently of the existence of its NMR assignment and even in the absence of structural information. Furthermore, it may complement high-resolution data to provide an independent validation of the reorientational time obtained in such analyses.

For both investigated proteins, the experimental low field relaxation rate values are significantly smaller than the theoretic

cal predictions by CORMA. This is an interesting result that could not have been guessed from water proton relaxation dispersion measurements, because the latter depend on the proton exchange rates, on the number of trapped water molecules, and on their exchange time in a covariant way.^{40,43,49} On the contrary, using this approach, the ratio between experimental and theoretical low field relaxation rates can be taken as a direct measure of the collective S_C^2 parameter in a model-free description of protein dynamics.

These estimates of S_C^2 may seem somewhat on the low side for those who are familiar with S^2 values in proteins.^{1–3,27} However, while normally these values are related to reorientation of internuclear vectors such as the backbone NHs, here we deal with all kinds of proton–proton interactions, including long-range ones, and these are certainly more sensitive to internal motions. Even short-range interactions such as those within a methylene group may be heavily influenced by local motions if the methylene group belongs, for instance, to the side chain of a surface residue. NMR studies on ¹⁵N-labeled HEWL showed that although main-chain amide S^2 are greater than 0.80 for the majority of residues, 15% of the residues have S^2 values between 0.5 and 0.8, and squared order parameters derived for the side chains range from 0.05 to 0.9.²⁷ Residues at the protein surface showed a side-chain S^2 below 0.3.²⁷ Furthermore, it has been shown that methyl group S^2 order parameters can be expressed as a function of contacts of the methyl carbon with respect to the neighboring atoms in combination with the number of consecutive mobile dihedral angles, n , between the methyl group and the protein backbone.²⁸ S^2 values smaller than 0.8 are common for methyl groups of valine, threonine ($n = 2$), leucine ($n = 3$), and methionine ($n = 4$).²⁸ With these considerations in mind, we suggest that a collective S_C^2 of 0.70–0.80 should be considered as normal for a well-behaved, “rigid” globular protein.

From these considerations, S_C^2 is also expected to increase with the molecular weight for globular proteins, as the relative number of surface residues, with larger side chain mobility, decreases. The accuracy of the S_C^2 value, at variance with that of the rotational correlation time, is however limited depending on the accuracy of the model used to interpret the collected experimental data. Its value is anyway still informative on the foldedness and degree of internal mobility of the investigated system.

The fit provides a high field plateau value that is about 0.2% and 2% of the low field value for HSA and HEWL, respectively, corresponding in both cases to a few s^{-1} . The essential independence of α from the reorientation time of the protein is an expected but important result for regularly folded proteins, as α should account for the $1 - S_C^2$ term relative to fast local motions that are likely independent of the protein size. Its value should be given by the missing 20–30% of $\langle E^2 \rangle$ (for all protons but methyl protons) times $J_1(\omega, \langle \tau_f \rangle)$, where $\langle \tau_f \rangle$ is the average correlation time modulating fast local rearrangements. The values of α and $1 - S_C^2$ set an order of magnitude estimate for $\langle \tau_f \rangle$ of about 0.5 ns.

This estimate of $\langle \tau_f \rangle$ is obtained in the assumption that all protons are modulated with the same average correlation time. Actually, it is possible that some protons are modulated by

(47) Bertini, I.; Luchinat, C.; Parigi, G. *Solution NMR of Paramagnetic Molecules*; Elsevier: Amsterdam, 2001.

(48) Palmer, A. G., III. *Chem. Rev.* **2004**, *104*, 3623–3640.

(49) Halle, B.; Denisov, V. P.; Venu, K. *Biol. Magn. Reson.* **1999**, *17*, 419–483.

longer τ_f , whose contribution to α is compensated by other protons modulated with smaller τ_f . However, it is difficult to figure out a small number of nuclei with large τ_f values, as the latter are expected to be roughly proportional to the number of nuclei undergoing collective motions. Of course, these motions do not exclude the simultaneous presence of more restricted motions in the <100 ps time scale, detected by heteronuclear relaxation at high field and essentially undetectable by our approach.

Conclusions

A theoretical model describing the collective protein proton relaxation rates has been developed, applied to the analysis of directly detected protein proton relaxation dispersions, shown to be general, and tested on two globular proteins of different sizes. It is shown that this analysis provides information on protein dynamics and protein aggregation, as it reveals a good sensitivity to oligomerization equilibria. Furthermore, it allows a straightforward definition of a collective order parameter, S_C^2 , which does not coincide with, but rather complements, that derived from high-resolution NMR relaxation analysis. A fast method for the estimation of this S_C^2 has been described, based on a complete relaxation matrix calculation at low magnetic field performed once for all, besides the fit of the experimental data. In fact, calculations on a number of different protein structures show that the theoretical values for low field relaxation rates in the absence of any local motion can be easily estimated, once the τ_R value is determined from the position of the collective relaxation dispersion. Since the relaxation rate distribution is very similar for all well folded proteins, the method is still valid even if the structure of the protein under investigation is unknown; on the other hand, the method can clearly indicate whether a protein is unfolded or partially unfolded from the obtained very low S_C^2 value, which is only a qualitative value in these cases, independently on the correctness of the assumed relaxation rate distribution.

Such a protocol can be applied to any protein sample, even without knowledge of its molecular weight, NMR assignment, and isotope enrichment. The protein could be for example isolated from an organism in the absence of genomic information. The present limitations of the method are an upper limit for the size of the protein of about 60–70 kDa and a protein concentration of about 40 mg/mL in 0.5 mL of D₂O solution. The size limit originates from the current upper limit in the time needed to cycle between relaxation and detection fields, which prevents the possibility of observing relaxation rates larger than approximately 2000 s⁻¹. Foreseen instrumental improvements should move the limit to about 100 kDa. As far as sensitivity is concerned, routine use of this proposed protocol can be anticipated even for samples with reduced concentration already with the present configuration. Sizable improvements in the sensitivity are foreseen for the near future,¹⁵ permitting the collection of protein proton magnetization decays for proteins in submillimolar concentrations, i.e., presumably at least a factor of 3 smaller with respect to the concentrations used in the present study.

Acknowledgment. Discussions with Prof. Ivano Bertini and David A. Case are gratefully acknowledged. The help of Dr. Andrea Giachetti for the MD calculations is also acknowledged. This work was supported by the European Commission (Contract HPRI-CT-2001-50028, Contract Bio-DNP 011721, Contract Ortho and para water 005032, and Contract LSHB-CT-2005-019102), by MIUR-FIRB (Contract RBAU013NSB), and by Ente Cassa di Risparmio di Firenze.

Supporting Information Available: CORMA calculations for increasing magnetic fields. Best fit of simulated relaxation dispersion data, aimed at the definition of the correct spectral density to be used. Equations used in the fit of the magnetization decays. Table of best fit collective protein proton relaxation rates for HEWL and HSA.

JA0633417